

# Environmental parameters measurement for an undersea neutrino telescope

N. Palanque-Delabrouille<sup>1</sup>

<sup>1</sup>DSM/DAPNIA, CEA/Saclay, 91191 Gif-Sur-Yvette CEDEX, France

*On behalf of the ANTARES Collaboration*

## Abstract

The ANTARES collaboration has completed an extensive series of measurements and samplings covering all relevant aspects in order to ascertain the adequacy of the site which has been selected for the deployment and the operation of an undersea neutrino telescope. Results of these investigations which include a climatological study of the area, a survey of the sea floor, measurement of current speed, and a detailed study of the optical properties of the site, are presented.

## 1 The ANTARES site

The chosen site for the deployment of a  $0.1 \text{ km}^2$  undersea neutrino detector is located 20 nautical miles off the coast from Toulon, in the Mediterranean sea ( $42^\circ 50' \text{ N}$ ,  $6^\circ 10' \text{ E}$ ), at a depth of  $\sim 2500 \text{ m}$ .

**1.1 Weather conditions** Weather conditions on the site have been studied using available meteorological data which include wind speed and direction from the Porquerolles Island as well as wave height records on a neighboring site. Deployment operations require sea conditions such that the wave height is less than 1.5 m and the wind speed less than 25 knots. The analysis of the available 4 years of data results in the following average occurrence of 3 consecutive days with favorable sea conditions: less than 5 such periods per month from October to April, and more than 5 such periods per month from May to September.

**1.2 Inspection of the sea floor** A detailed survey of the sea floor has been performed using the submarine NAUTILE, from IFREMER. It displays neither topographical accidents (steps, rocks...) nor the presence of any important debris in the area we have retained. During the same series of dives, cores from the bottom were recovered. They consist in a solid mud which is an adequate floor for the deployment of the mechanical structures we envision.

**1.3 Sea parameters** Conductivity, temperature, and current speed have been monitored during the 14 sea campaigns we have conducted for the last three years, giving an overall view of their seasonal variations. Salinity and temperature are extremely stable :  $33.65 \text{ ‰}$  and  $13.2 \text{ deg}$ . Current speed which is in average 2 to 3 cm/s never exceeded 17 cm/s. Nevertheless, values as high as 30 cm/s are considered in the design of the detector lines, since it has an impact, for instance, on their mechanical lay-out and the minimum distance we can set between adjacent lines.

## 2 Optical properties of the ANTARES site

A special emphasis has been put on the study of the optical properties of the site. Indeed, these properties contribute to determine the design and the performance of the detector. Four different measurement systems have been designed by the ANTARES collaboration and utilized several times over a period of about three years in order to quantify the parameters of light transmission, the deep sea background light, and the fouling on glass surfaces. They are detailed hereafter.

**2.1 Fouling on glass spheres** Fouling occurs on the modules, due to sedimentation and possibly to the growth of bacteria on the surfaces. The measurement of the fouling rate is crucial for a long-term project planning to leave optical modules immersed for several years. In order to complement the previous test of fouling near the upper pole of optical modules (de Botton, 1997) which showed that as much as 40% of the transmission efficiency could be lost at the upper pole of a module after 30 days of immersion, a long term

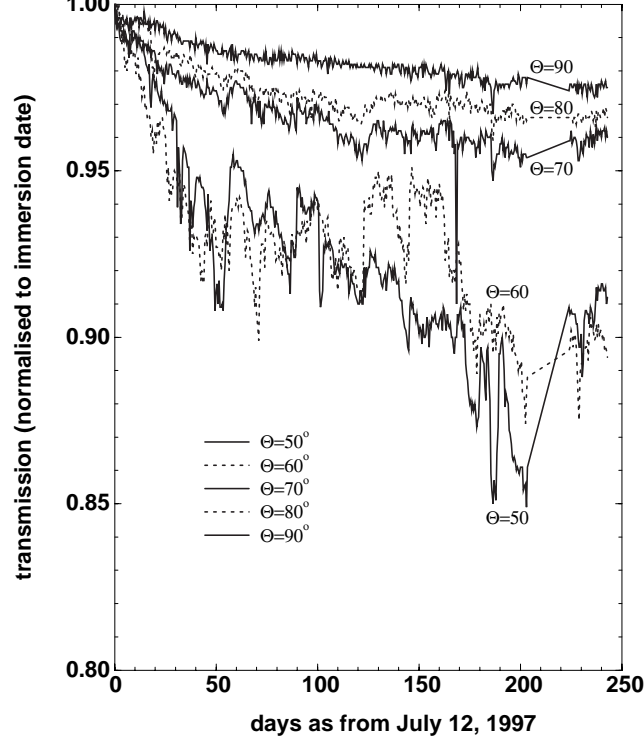


Figure 1: Fouling measurements near the equator of a glass sphere.

measurement has been performed in order to study the loss of transmission in regions close to the equator of a glass sphere (see figure 1). As expected, the fouling is significantly reduced for polar angles larger than 50 degrees. At the equator, the fouling produces a loss of transmission of 1.5% after eight months of immersion. This number is therefore an upper limit of what the fouling is expected to be on the actual detector whose optical module axes will be oriented at a polar angle of 135 degrees.

**2.2 Background light** The design of the detector architecture as well as the trigger logics and the electronics should take into account the presence of background light pulses which will also affect the quality of the reconstruction of the events. Detailed investigation of the phenomenon and of its seasonal variations on the ANTARES site has been pursued.

Background light on an optical module mounted with an 8'' photomultiplier tube displays three distinct components:

- a  $\sim 20$  kHz contribution from  $\beta$ -decay of  $^{40}\text{K}$ , constant in time,
- a component slowly varying on typical time scales of a few hours and which can reach up to a 20 kHz rate,
- short bursts of a few ms rise-time which decay typically within 1 or 2 seconds, with counting rates reaching tens of MHz. These bursts are probably due to the light emission of living organisms in the deep sea.

We observed a strong correlation of the bioluminescence rate (defined as the proportion of time a given optical module exhibits a counting rate which exceeds 200 kHz — rate above which the acquisition electronics starts to be affected by significant dead time) with the current speed. The actual dependence exhibits also a seasonal variation, as illustrated in figure 2.

We have studied the correlations of the background light signals seen by optical modules as a function of their separation. Short intense bursts are observed simultaneously only by neighboring optical modules (separation smaller than 1.5 meter). On the contrary, even when they are 40 meters apart, two optical modules sense the same variations of the slow component (see figure 3).

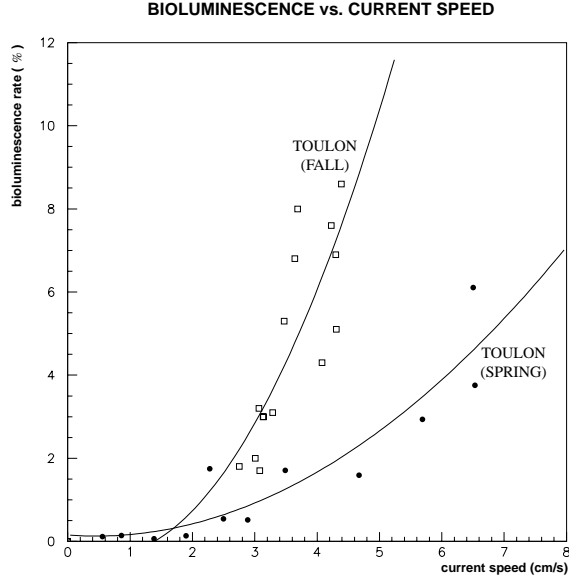


Figure 2: Correlation between the bioluminescence burst activity and the current velocity for two different series of measurements.

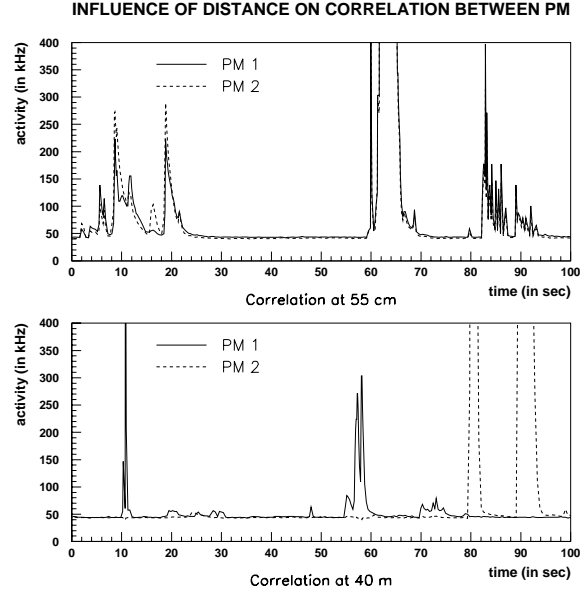


Figure 3: Example of time streams illustrating the strong correlation between the counting frequencies of modules located 55 cm apart and the negligible correlation for modules 40 m apart.

On average, the counting rate of an optical module exceeds 200 kHz a few percent of the time, depending on the current speed and possibly the season. When integrated over the measured distribution of counting rates, the dead time induced on the electronics for the whole detector is less than a 5% inefficiency, randomly distributed over the detector because of the absence of correlation we have mentioned previously for distant modules.

The counting rates given above were measured with a detection threshold of an average 0.3 photo-electron. Setting the threshold to 2 photo-electrons suppressed the background light by a factor of one hundred. This however would also considerably reduce the expected signal from muons. A safer solution to reduce the contribution of background light hits to physics events is to require tight coincidences between neighboring optical modules, as will be done for the hardware trigger. This indeed lowers the total rate due to  $^{40}\text{K}$  and the slow component down to  $\sim 10$  Hz for two optical modules located 1.4 m apart and both pointing in the same direction. For the actual configuration of the final detector, the coincidence rate from background light will be even lower.

**2.3 Light transmission** Different combinations of the two components of light transmission, absorption and scattering, have been studied in situ using two measuring systems. These measurements are described more thoroughly in (Palanque-Delabrouille, 1999), these proceedings.

In the first set-up, the effective attenuation length was measured using a collimated light source and an 8" photomultiplier tube located at a variable distance from the source. The intensity of the source was adjusted so as to yield a constant current on the phototube. We thus measured an effective attenuation length at a

wavelength of 466 nm of:

$$\lambda_{\text{att, eff}} = 41 \pm 1 \text{ (stat.)} \pm 1 \text{ (syst.) m (December 97)} \quad (1)$$

The second set-up measured the arrival time distribution of photons emitted by an isotropic LED source and detected either 24 m or 44 m away by a 1" photomultiplier tube. The comparison of the integrated number of counts for the two distances yield, in a similar manner as previously, an estimate of an effective attenuation length:

$$\lambda_{\text{att, eff}} = \begin{cases} 60.0 \pm 0.4 \text{ (stat.) m (July 98)} \\ 52.2 \pm 0.7 \text{ (stat.) m (March 99)} \end{cases} \quad (2)$$

These estimates would be lower by about 10% if a collimated source had been used instead of an isotropic one. The remaining difference, however, is significant and we might infer a slight seasonal variation of the water transmission. For this second set-up, the tail of the arrival time distribution is negligible as compared to the peak of “direct” photons, implying that scattering is quite negligible in the site under study: 95% of the photons arrive with a delay smaller than 10 ns for the 24 m distribution (45 ns for the 44 m one). Figure 4 shows one set of measurements of the arrival time distribution.

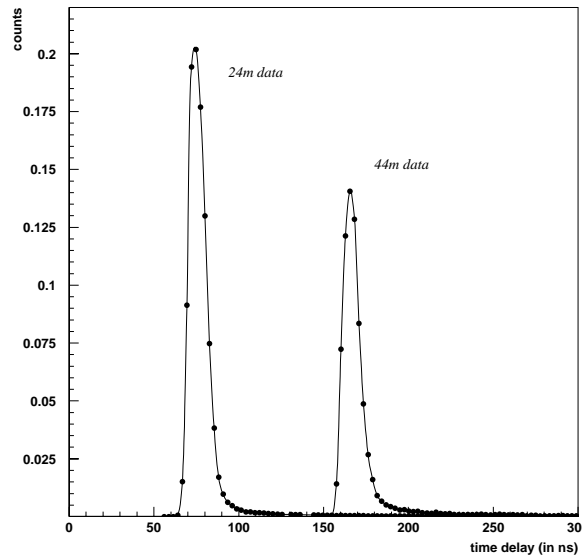


Figure 4: Distribution of photons arrival times for two source-deflector distances: 24 m and 44 m.

A fit to the measured distributions can yield the individual contributions from absorption and scattering. The absorption length is in the range [55-65] m and the scattering length at large angle exceeds 200 m.

## References

- de Botton, N. 1997, ICRC 97 proceedings, Durban  
Palanque-Delabrouille, N. 1999, ICRC 99 proceedings, HE 6.3.18